

CONCEPTUAL DESIGN OF RAPID CYCLING BOOSTER FOR ACCELERATOR FACILITY FOR CANCER THERAPY

V.A. Kiselev, E.B. Levichev, V.V. Parkhomchuk, Yu.A. Pupkov, V.A. Vostrikov, BINP SB RAS, Novosibirsk, Russia

Abstract

The rapid cycling booster synchrotron is used as pre-accelerator for carbon ion facility for cancer therapy. Booster provides about 10^{10} carbon ions per second at extraction energy 30 MeV/unit, at a repetition rate of 10 Hz. At the same time the booster can be used for acceleration of protons and delivers about 10^{12} protons per minute at maximum extraction energy of 250 MeV in separate irradiation port.

INTRODUCTION

At BINP SB RAS, the carbon ion synchrotron with electron cooling has been proposed for cancer treatment [1-3]. The electron cooling application enables as significantly decrease aperture of main synchrotron as storage of high intensity ion beams. The injection part of facility placed inside the main synchrotron includes a pre-injector and rapid cycling booster synchrotron with maximal energy of $^{12}\text{C}^{+4}$ carbon ions 30 MeV/u. The beam intensity is up to $2 \cdot 10^9$ particles per cycle.

The 10 Hz intermediate booster provides possibility of pre-injector different types application. The base scheme includes two ECR ion sources and linear accelerator with energy 6 MeV/u. Reducing of pre-injector energy leads to complication of booster power supplies and RF system. An alternative tandem accelerator with terminal voltage about 2 MV keeps acceptable booster design.

The main synchrotron operation assumes the ion beam storage and cooling at injection energy during 1 s. At low energy the equilibrium emittance of cooled high intensity beam is limited by space charge tune shift. So, the main synchrotron aperture reducing is sufficient only with increasing of injection energy.

The most part of facility operation time, during main synchrotron acceleration cycle and extraction, the injector system is unused. The magnet rigidity of booster corresponds to proton energy 250 MeV. The beam line from booster for the independent passive proton treatment can be additionally installed.

In further development the combination of intermediate booster and main synchrotron with electron cooling can be simply modified for the production and accumulation of intense beams of isotopes that decay by positron emission. Such beams application provides treatment with online PET monitoring of delivered doze.

BOOSTER SYNCHROTRON

Lattice

The magnet lattice consists of eight identical combined functions rectangular magnets and has no quadrupole

lenses. The magnet has the FDF structure where focusing (F) and defocusing (D) sectors deflect the beam 12.64 and 19.72 degrees, respectively. The n -value of the magnet is determined as ± 7.56 . At the straight drifts the sextupole lenses, RF cavity and elements of injection/extraction are placed. The main parameters of the booster synchrotron are summarized in Table 1. The layout of booster is shown in Figure 1. The optical functions of the booster synchrotron are presented in Figure 2.

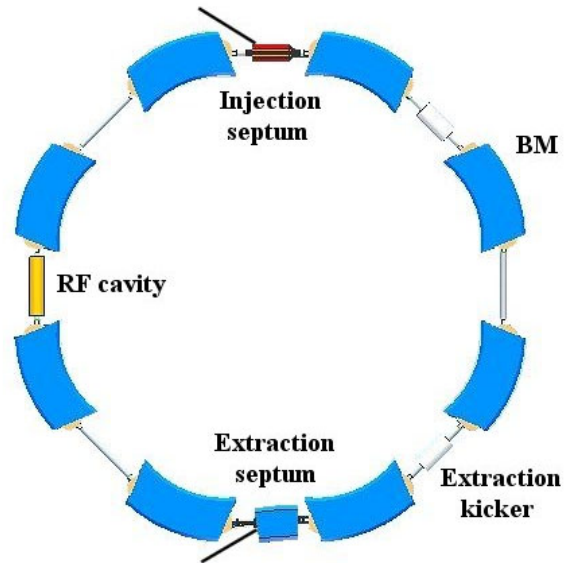


Figure 1: Layout of booster.

Table 1: Main booster parameters

Particles	$^{12}\text{C}^{+4}$
Injection energy, MeV/u	6
Extraction energy, MeV/u	30
Magnet rigidity, T·m	2.4
Circumference, m	29.7
Revolution frequency, MHz	1.14/2.5
Magnet field inj/max, T	0.53/1.2
Repetition rate, Hz	10
Tunes ν_x/ν_y	1.76/1.3
Max. β -function x/y, m	3.2/5.8
Max. dispersion, m	1.6
Momentum compaction factor	0.31
Transition energy, γ_{tr}	1.79
Chromaticity ξ_x/ξ_y	-1.18/-1.35

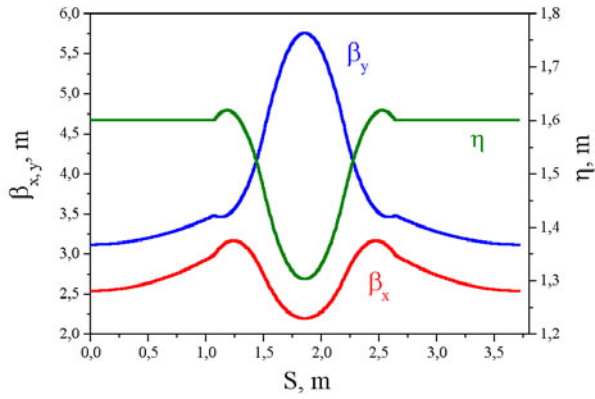


Figure 2: Optic functions of booster.

Chromaticity

For rapid cycling accelerators eddy currents induced in vacuum chambers are typically the dominant source of sextupole field perturbations. The maximal value of sextupole component is $K_2 = 0.85 \text{ m}^{-3}$ and 2.25 m^{-3} for $^{12}\text{C}^{+4}$ and protons accordingly. The parameters of accelerating cycle are following: $B_{min} = 0.53$ and 0.178 T , $B_{max} = 1.2 \text{ T}$, $(\partial B/\partial t)_{max} = 21$ and 32.1 T/s , thickness of vacuum chamber wall is 1 mm ; average magnet gap is 50 mm . The natural chromaticity $\xi_{x,y}$ is -1.18 and -1.35 accordingly. In Fig.3 the dependence of total chromaticity on time is shown.

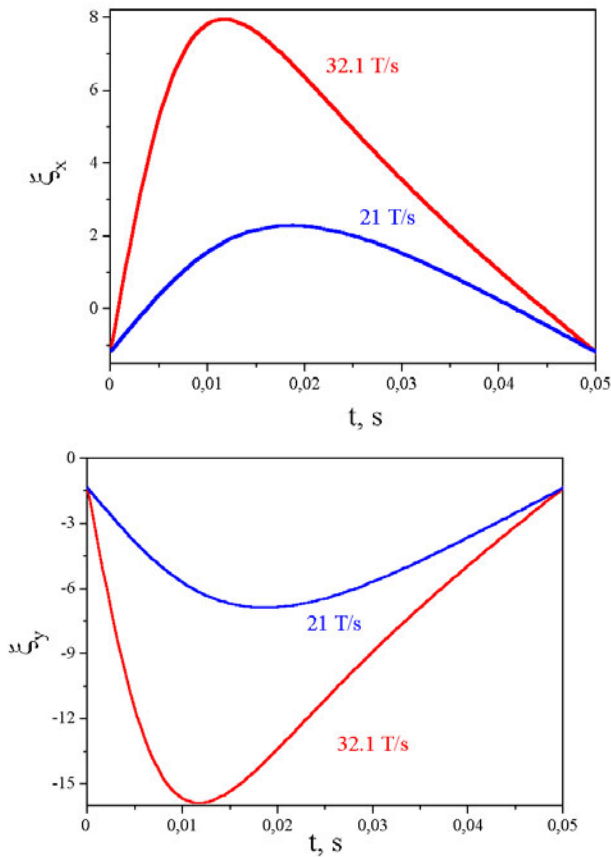


Figure 3: Dependence of total chromaticity on time for different accelerating cycles.

Bend Magnet

The booster dipole with curvature radius 2.0 m is an H-type design. The dipole has been curved to account for the 152 mm beam sagitta. The half yokes are stacked, put under compression and glued. The two halves can then be welded or bolted to form the complete yoke. The pole profile is calculated in two dimensions and the end fields will be compensated by shims added at the time of the measurements. This is preferred to a uniformly-distributed correction of the pole profile because the lattice functions change appreciably along the magnet. The laminations have thickness of 0.5 mm and are covered by gluey layer.

In the Tab. 2 the basic parameters of bend magnet are presented. Figure 4 shows the schematic view of the laminations. The laminations for F and D sectors are identical. The excitation coil contains 48 turns hollow copper conductor of cross section $21 \times 18 \text{ } \varnothing 9 \text{ mm}$. All turns are connected in series.

Table 2: Parameters of Bend Magnet

Number of magnets	8
Bending angle	45°
Bending radius, m	2.0
Magnet field min/max, T	0.13/1.2
Effective magnetic length, m	1.571
Average gap, mm	50
Homogeneity region vert/hor, mm	$\pm 24/\pm 40$
Non-homogeneity in that region, not worse	$4 \cdot 10^{-4}$
Saturation level at Max current	6
Total number of turns/dipole	48
Peak current, A	1015
Frequency	10
Copper conductor size, mm	$21 \times 18, \varnothing 9$
Active DC resistance (at 30°C), mOhm	11.3
Total inductance, mH	24.2
Peak current density, A/mm^2	3.3
Peak power consumption per dipole, kW	11.6
Average power consumption per dipole, kW	4.74
Total flow rate per dipole, l/min	3.5
Copper weight, kg	200
Total weight, t	3.7

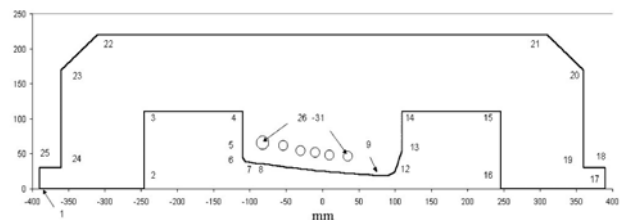


Figure 4: Lamination.

Figure 5 shows the two dimensional magnetic field distribution obtained by numerical analysis. The horizontal axis shows the radial distance r_i from the design orbit and the vertical axis shows the deviation of the magnetic field strength $\Delta B/B$ from the design value. As shown in the figure, the difference, between the calculated and design values, is smaller than 0.02% at even the magnetic field of 1.2 T for the horizontal width of 80 mm.

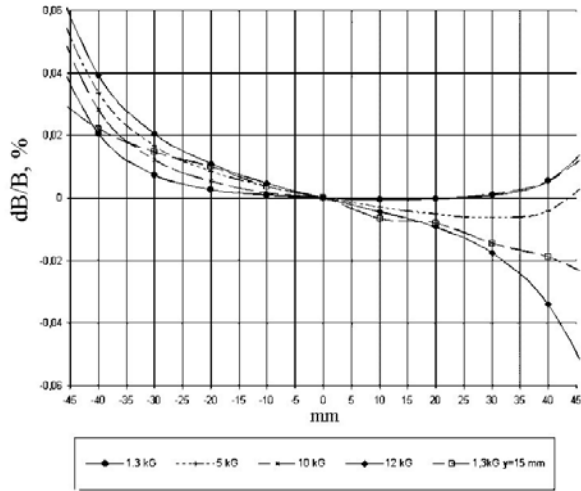


Figure 5: The homogeneity of field in bend magnet.

The transition region between focusing and defocusing sectors is a source of nonlinear magnetic fields. These perturbations appear at high field due to saturation of prominent ends of poles. For prevention of such effects the pole smoothing or insertion of block without gradient can be applied. The length of transition area is equal of

average magnet gap. The estimated tune shifts for insertion case are $\Delta\nu_x = -6 \cdot 10^{-3}$, $\Delta\nu_y = -1.23 \cdot 10^{-2}$ and can be neglected. For smoothing case the tune shift values are twice smaller.

Injection & Extraction

The booster applies a multi-turn injection in horizontal plane. The injection is carried out by means of a shift of equilibrium orbit. Two pairs of bump magnets generate such orbit distortion. In the case of tandem pre-accelerator $^{12}\text{C}^{+2}$ ions beam is injected by using multi-turn charge exchange injection scheme.

The fast extraction from the booster is performed by a kicker magnet and a septum magnet with the bending magnet between.

CONCLUSION

The rapid cycling booster synchrotron with multi-turn injection and fast extraction is proposed at BINP SB RAS in frames of the carbon accelerator facility for cancer treatment. The magnetic lattice of booster bases on the combined function dipole magnets. Also the booster provides beam intensity required for independent proton treatment.

REFERENCES

- [1] M. Kumada et al., PAC 05, Knoxville, 1108.
- [2] V. Parkhomchuk et al., COOL05, Galena, AIP Conf.Proc. 821:365-369, 2006.
- [3] E. Levichev et al., RUPAC06, Novosibirsk.